Hindawi
Discrete Dynamics in Nature and Society
Volume 2022, Article ID 8677470, 14 pages
https://doi.org/10.1155/2022/8677470

Research Article

On Complex Dynamics of Differentiated Products: Cournot Duopoly Model under Average Profit Maximization

S.S. Askar

Department of Statistics and Operations Research, College of Science, King Saud University, P.O. Box 2455, Riyadh 11451, Saudi Arabia

Correspondence should be addressed to S.S. Askar; saskar@ksu.edu.sa

Received 7 November 2021; Accepted 14 February 2022; Published 8 March 2022

Academic Editor: Lei Xie

In this paper, some important dynamic characteristics such as multistability and synchronization phenomena are investigated for a game of an economic Cournot duopoly whose time evolution is received by the iteration of a noninvertible map in the plane. In the asymmetric case, the equilibrium points of game's map are calculated, and their stability conditions are obtained. The obtained results show that the Nash equilibrium point loses its stability through flip bifurcation. Under some restrictions, the map's coordinate axes form an invariant manifold, and hence their dynamics are studied based on a one-dimensional discrete dynamic map. In the symmetric case where both firms are identical, the map has the property of symmetry, and this implies that the diagonal $q_1 = q_2$ forms an invariant manifold and therefore synchronization phenomena occur. Global analysis of the behavior of the noninvertible map is carried out through studying critical manifolds of the map that categorize it as $Z_4 - Z_2 - Z_0$ type. Furthermore, global bifurcation of the basins of attraction is confirmed through contact between the critical curves and the boundaries of escaping domain.

1. Introduction

Dynamic economic games whose evolutions has been depended on discrete time maps have attracted many researchers due to the interesting dynamic behaviors and bifurcations types occurring in such maps. Analyzing the dynamic characteristics of such maps has been dated at least to [1] by Puu who passed away in 2020 after enriching this direction with many useful books and papers. In the current paper, we focus on a special type of these maps that are known as duopoly maps. In duopoly game, the market possesses only two competing firms (or players) whose target is seeking the optimal quantities in the case of Cournot by maximizing their profits, or seeking the optimal prices in the case of Bertrand. Cournot, the French economist who started the core of such kind of games in 1838, introduced a duopoly model adopting quantities as decision variables. Later in 1880s and based on Cournot model, Bertrand suggested his model known as Bertrand model and considered prices as competitive means. In 1950, the Nash equilibrium point detected by the famous American mathematician John Nash has been raised in the equilibrium theory of noncooperative games. In general, this theory provided research with significant tools in studying oligopoly models. As a result, Nash point became important aspect in studying such models and was found in several Cournot and duopoly games. Indeed, one has to highlight game theory as an important tool of applied mathematics that was used and adopted to study the interaction among players in those economic games. It has been used in studying the strategic interactions among rational competitors and decision-makers. Game theory was extensively developed in the 1950s by many scholars and was explicitly applied to all fields of social science, as well as logic, biology, economics systems, and computer science. Recently, the theory of game has extensively been applied in economics for studying competitions among competing firms. Even though static equilibrium analysis of such games is limited and has not provided valuable information on games' evolutions, it has been investigated by many researchers (see, for example, [2]). Studying the game evolution through dynamics gives more information on the stability/

instability of Nash equilibrium, the types of bifurcations by which it loses its stability, and the topological properties of basin of attraction in the phase plane. Rand [3] was the first to introduce and analyze some of these dynamic characteristics.

Firm in duopoly competition simultaneously chooses its decision or strategy taking into account two important factors: its own actions and actions by its competitor. In literature, several works have been reported for studying the dynamic characteristics of duopoly games. These dynamic characteristics included bifurcation and its types, either flip or Neimark–Sacker; peculiar shapes of attractive basins for attracting sets and chaotic attractors; and multistability phenomena. Furthermore, studying such games requires adopting specific kinds of utility consumer preferences. The most popular one that is well-known as Cobb–Douglas utility was adopted in many studies in literature. The reason is that Cobb–Douglas utility is a particular functional form of the production function. It has been widely used to represent the technological relationship between the inputs and outputs that can be produced by those inputs. Moreover, literature reported many other utility functions such as constant elasticity of substitution (CES) and Singh and Vives utility. One can get more information and properties of those utilities from literature ([4–10]).

The dynamic characteristics of duopoly models are complex and reveal interesting information on their evolutions. Therefore, many interesting results on these complex dynamics have reported many interesting results on the stability of Nash equilibrium point of these games and opened the routes to attract many researchers. Some related works and results for these models are reported here. For example, a game of two competing firms whose decision variables are different (Cournot duopoly game) has been analyzed in [11]. Other studies on duopoly and triopoly in which firms seek the optimality of production have been introduced and investigated in ([12–14]). In [15], a Cournot duopoly game whose players are rational, adopting bounded rationality rule and seeking maximization of their relative profits, has been introduced and analyzed. Using a theoretical framework, a Cournot–Bertrand game has been formalized in [8]. In [16], Cournot–Bertrand model has been studied by Naimzada et al. using a two-dimensional discrete linear map. They focused on investigating the dynamic characteristics of Nash equilibrium points and its instability through two types of bifurcations. Additionally, analyzing the game's evolution requires representing it by a discrete time map so that firms can update of their productions. This requires some kinds of adjustment rules. Literature has presented and reported many of these rules. The first rule among those rules which has been extensively adopted is known as bounded rationality. It has been deeply adopted in many studies for process of modeling discrete time maps representing the evolutions of these games. It is described as a gradient rule because it depends on firms' marginal profits and requires firms to carry out an estimation of their marginal profits to determine whether they increase or decrease, so they can update their outputs next period of time. There are also other mechanisms which have been used in the modeling process such as tit-for-tat rule and local monopolistic approximation mechanism ([17–27]).

Based on a linear inverse demand functions and adopting the bounded rationality mechanism, a Cournot duopoly game with players seeking the maximization of their average profits is introduced and analyzed in this manuscript. Most firms do not rank profits as the major goal. The work of modem firms is so complex that they do not think merely about profit maximization. The basis of the difference between the objectives of the neoclassical firm and the modem corporation arises from the fact that the profit maximization objective relates to the entrepreneurial behavior while modem corporations are motivated by different objectives because of the separate roles of shareholders and managers. Due to the above discussion, we have introduced a general case with different objectives. The game is described by a nonlinear discrete dynamic map that possesses four equilibrium points, three of which are boundary points, and the fourth is an interior point and coincides with Nash equilibrium point. We use in this manuscript local and global analysis to investigate the dynamics of these equilibrium points. The analysis shows that Nash point loses its local stability through flip bifurcation. The structure of the game's map shows that it is being attracted to the origin, and hence its coordinate axes form an invariant manifold. Consequently, the map's dynamics are studied by a one-dimensional map conjugating the famous logistic map. It is also shown that under some restrictions, the synchronization phenomena are studied and show that the diagonal in map's phase plane forms an invariant manifold. Furthermore, our findings show that the game's map is noninvertible and its phase plane is divided into three zones that make it belong to $Z_4 - Z_2 - Z_0$ type.

The sections in the current paper are summarized as follows. In Section 2, the discrete form of the game's map is introduced. The equilibrium point and its stability are investigated both analytically and numerically through local analysis in Section 3. In Section 4, the invariant manifold is studied. The basin of attraction and critical curves are analyzed in Section 5. In Section 6, the global analysis and synchronization phenomena are investigated based on some numerical experiments.

2. The Model

Suppose an economic market consisting of two competing firms (or players) whose decision variables are quantities, q_1 and q_2. Both firms adopt linear inverse demand functions given by

$$\begin{aligned} p_1 &= a - q_1 - bq_2, \\ p_2 &= a - q_2 - bq_1. \end{aligned} \tag{1}$$

The horizontal differentiated products mainly refer to difference in extrinsic features between the products, like color and shape. Such differentiation mostly adapts to differences in consumer preferences. In (1), the parameter b refers to the degree of horizontal product differentiation that is taken in the interval $[0, 1]$. For $b = 0$, each firm behaves as a monopoly player due to the independent varieties between firms' products. $b = 1$ means that both products are perfect substitutes or

are homogenous, and hence $p_1 = p_2$. In this paper, we focus on the case of $b \in (0, 1)$. The parameter a denotes maximum price in market. Suppose that the competing firms adopt different nonnegative marginal costs and hence their total costs are taken as $C_i(q_i) = c_i q_i, i = 1, 2\ (c_1 \neq c_2)$. Now, the total profit for each firm takes the following form.

$$\begin{aligned} \pi_1 &= (a - c_1 - q_1 - bq_2)q_1, \\ \pi_2 &= (a - c_2 - q_2 - bq_1)q_2. \end{aligned} \tag{2}$$

Unlike many studies in literature, the current game assumes that both firms focus on maximization of their average profits rather than profits only. The average profits then become

$$\begin{aligned} \varphi_1 &= \pi_1 + r_1\pi_2, \\ \varphi_2 &= \pi_2 + r_2\pi_1. \end{aligned} \tag{3}$$

The parameter $r_i, i = 1, 2$, where $0 < r_i < 1$, is directly used to measure altruism. That is to say, it explains the firms' care of average performance. When $r_i = 0, i = 1, 2$, it means firms give care to their own profits only. Substituting (4) into (5), one gets

$$\begin{aligned} \varphi_1 &= (a - c_1)q_1 + r_1(a - c_2)q_2 - q_1^2 - r_1q_2^2 - b(1 + r_1)q_1q_2, \\ \varphi_2 &= (a - c_2)q_2 + r_2(a - c_1)q_1 - q_2^2 - r_2q_1^2 - b(1 + r_2)q_1q_2, \end{aligned} \tag{4}$$

and then the marginal average profits $(\partial\varphi_i/\partial q_i, i = 1, 2)$ become

$$\begin{aligned} \frac{\partial\varphi_1}{\partial q_1} &= a - c_1 - 2q_1 - b(1 + r_1)q_2, \\ \frac{\partial\varphi_2}{\partial q_2} &= a - c_2 - 2q_2 - b(1 + r_2)q_1. \end{aligned} \tag{5}$$

Maximizing the average profits requires firms to know some characteristics of market and the nature of competition. Knowing the characteristics of market needs complete information on the market and the strategies of firms' rivals, and these become impossible. Therefore, firms believe that updating output productions requires watching the changes taking place in the marginal average profits. That is to say, if $\partial\varphi_i/\partial q_i > 0$, this means firms will increase their production next period of time; otherwise, they decrease productions or become naive. Accordingly, firms estimate production based on bounded rationality rule that has the following form.

$$q_i(t + 1) = q_i(t) + \nu_i(q_i)\frac{\partial\varphi_i}{\partial q_i}; \quad i = 1, 2. \tag{6}$$

Adopting bounded rationality rule makes us assume that $\nu_i(q_i) = \nu_i q_i$, $i = 1, 2$, where $\nu_i > 0$, $i = 1, 2$ is known as the speed of adjustment parameter. This gives $(q_i(t + 1) - q_i(t)/q_i(t)) \propto \partial\varphi_i/\partial q_i$ which makes relative production directly proportional to the firms marginal average profits. Equation (6) possesses some important characteristics that can be found in literature ([25–28]). Substituting (5) into (6), one simply has a two-dimensional discrete map that will be used throughout the manuscript to discuss the game's repetition (or evolution).

$$T(q_1, q_2): \begin{cases} q_1(t + 1) = q_1(t) + \nu_1 q_1(t)[a - c_1 - 2q_1(t) - b(1 + r_1)q_2(t)], \\ q_2(t + 1) = q_2(t) + \nu_2 q_2(t)[a - c_2 - 2q_2(t) - b(1 + r_2)q_1(t)]. \end{cases} \tag{7}$$

The parameter $t = 0, 1, 2, \ldots$ denotes time steps. Setting the fixed points' condition, $T(q_1, q_2) = (q_1, q_2)$ in (7), one has four fixed points given by

$$\begin{aligned} e_o &= (0, 0), \\ e_1 &= \left(\frac{a - c_1}{2}, 0\right), \\ e_2 &= \left(0, \frac{a - c_2}{2}\right), \\ e_* &= \left(\frac{2(a - c_1) - b(a - c_2)(1 + r_1)}{4 - b^2(1 + r_1)(1 + r_2)}, \frac{2(a - c_2) - b(a - c_1)(1 + r_2)}{4 - b^2(1 + r_1)(1 + r_2)}\right). \end{aligned} \tag{8}$$

3. Local Stability

In order to study the stability of the fixed points (8), we recall the Jacobian matrix at these points, and hence the following propositions are raised (their proofs are given in Appendix).

Proposition 1. *The point e_o is an unstable repelling node.*

Proposition 2. *The point e_1 is a stable point provided that $0 < \nu_1 < 2/a - c_1$ and $a - c_2 < b/2(1 + r_2)(a - c_1)$. It is an*

unstable saddle if $0 < \nu_1 < 2/a - c_1$ *and* $a - c_2 > b/2(1 + r_2)(a - c_1)$.

Proposition 3. *The point* e_2 *is a stable point provided that* $0 < \nu_2 < 2/a - c_2$ *and* $a - c_1 < b/2(1 + r_1)(a - c_2)$. *It is an unstable saddle if* $0 < \nu_2 < 2/a - c_2$ *and* $a - c_1 > b/2(1 + r_1)(a - c_2)$.

Proposition 4. *The point* e_* *that is called Nash point is locally stable provided that*

$$0 < 2A\nu_1 + 2B\nu_2 - 4AB\nu_1\nu_2 + b^2(1 + r_1)(1 + r_2)AB < 4,$$

$$A = \frac{2(a - c_1) - b(a - c_2)(1 + r_1)}{4 - b^2(1 + r_1)(1 + r_2)},$$

$$B = \frac{2(a - c_2) - b(a - c_1)(1 + r_2)}{4 - b^2(1 + r_1)(1 + r_2)}. \tag{9}$$

Proposition 5. *The point* e_* *loses its stability due to flip bifurcation only.*

The obtained results show that the stability condition of Nash point depends on the parameters a, b, c_1, c_2, r_1, r_2 and the speed of adjustment parameters ν_1 and ν_2. Some numerical experiments are carried out here to validate the theoretical results given above. As in many studies in literature, we keep our focus on studying the influences of speed parameters on the stability of Nash while fixing the other parameters. Let us suppose the set of parameters $a = 1, b = 0.35, c_1 = 0.4, c_2 = 0.3, r_1 = 0.7, r_2 = 0.5$, and $\nu_1 = 1$ (or $\nu_2 = 3.852$) on varying ν_2 (or on varying ν_1). Figures 1(a) and 1(b) show the one-dimensional period-doubling bifurcation diagram on varying ν_1 with respect to the two decisional variables q_1 and q_2. As one can see, both figures present flip bifurcation diagrams. In Figures 1(c) and 1(d), one can see the flip bifurcation on varying the speed parameter, ν_2. In Figure 1(e), the phase plane of period-8 cycle with Nash equilibrium point is depicted. Figure 1(f) shows a one-piece chaotic attractor. In Figures 1(g) and 1(h), a two-piece disconnecting chaotic attractor is given. In these figures the marginal costs are fixed.

4. The Invariant Manifold

Looking at the map (7), one can see that the point $(0, 0)$ is trapping the map. That is to say, if $q_1(t) = 0$ or $q_2(t) = 0$, one gets $q_1(t + 1) = 0$ or $q_2(t + 1) = 0$, and hence both coordinate axes become invariant axes for the map. Therefore, the invariant set made of the axes q_1 and q_2 forms an invariant manifold for T. Accordingly, the dynamics of the map (7) on the invariant axes can be described by the one-dimensional map given by

$$q_i(t + 1) = \left[1 + (a - c_i)\nu_i\right]\left[1 - \frac{2\nu_i}{1 + (a - c_i)\nu_i}q_i(t)\right]q_i(t), \quad i = 1, 2. \tag{10}$$

It is easy to see that the map (10) is topologically equivalent to

$$u_i(t + 1) = \mu_i u_i(t)(1 - u_i(t)), \quad i = 1, 2, \tag{11}$$

through the transformation given below.

$$q_i = \frac{1 + (a - c_i)\nu_i}{2\nu_1}u_i, \quad i = 1, 2, \tag{12}$$

and $\mu_i = 1 + (a - c_i)\nu_i$, $i = 1, 2$.

4.1. Dynamic Analysis. For equation (11), suppose the following function.

$$\sigma(u) = \mu u(1 - u). \tag{13}$$

Function (13) shows the logistic equation, and μ is the parameter responsible for its dynamics. It has a first derivative given by $\sigma(u) = \mu(1 - 2u)$. Its maximum value occurs at $\mu/4$ at the point $u = 1/2$. In addition, $\sigma(0) = 0$ and $\sigma(1) = 0$, which means that $\sigma(u) \in [0, 1)$ on the open interval $0 < \mu < 4$ and for all $u \in [0, 1]$. Moreover, it is easy to see that (11) has only two fixed points, that is, $\overline{u} = 0$ and $\overline{u} = 1 - 1/\mu$, where $\mu > 1$. Consequently, $\sigma(0) = \mu$, and then $\overline{u} = 0$ is stable if $\mu \in (0, 1)$ and unstable otherwise. The other fixed point $\overline{u} = 1 - 1/\mu$ is stable if $\mu \in (1, 3)$ and unstable if $\mu > 3$. In addition, one can see that the map (11) has two fixed points, $\overline{u} = 0$ and $\overline{u} = 1 - 1/\mu$, where $\mu > 1$. Hence, $\sigma(0) = \mu$, and then $\overline{u} = 0$ is stable if $\mu \in (0, 1)$ and unstable otherwise. The other fixed point $\overline{u} = 1 - 1/\mu$ is stable if $\mu \in (1, 3)$ and unstable if $\mu > 3$.

The simulation in Figure 2(a) presents a 1D bifurcation diagram on varying μ that confirms that the point $\overline{u} = 1 - 1/\mu$ is stable in $\mu \in (1, 3)$. In Figure 2(b) a cobweb diagram is given at $\mu = 2.99$ in the stability interval and shows a stable fixed point, while in Figure 2(c), an unstable behavior is plotted at $\mu = 3.75$, and hence the instability of the fixed point is confirmed.

Proposition 6. *Once the critical value* $\nu_i = 2/(a - c_i)$, $i = 1, 2$, *is reached, the trajectories of* T *starting on the invariant axes diverge when* $\nu_i \in (2/(a - c_i), +\infty)$, $i = 1, 2$.

Proof. The proof is straightforward as $\mu_i = 1 + (a - c)\nu_i$, and our discussion given above confirms the topological equivalence between the map (7) and (11) on which the trajectories of (11) diverge when $\mu_i > 3$, $i = 1, 2$. □

4.2. The Symmetric Case. In this subsection, the symmetric case $\nu_1 = \nu_2 = \nu, c_1 = c_2 = c$, and $r_1 = r_2 = r$ is studied. As one can see, the map T defined in (7) is symmetric. That is to say, its structure does not change if the decision variables q_1 and q_2 are swapped; i.e., $T \circ S = S \circ T$, where S: $(q_1, q_2) \longrightarrow (q_2, q_1)$. This means that the diagonal defined by $\Delta = \{(q_1, q_2)\colon\ q_1 = q_2\}$ forms an invariant manifold. It implies that the dynamics of any trajectories starting on the diagonal $(q_1(0) = q_2(0))$ will get back to the diagonal for every t. In this case, the dynamic behavior of map (7) under

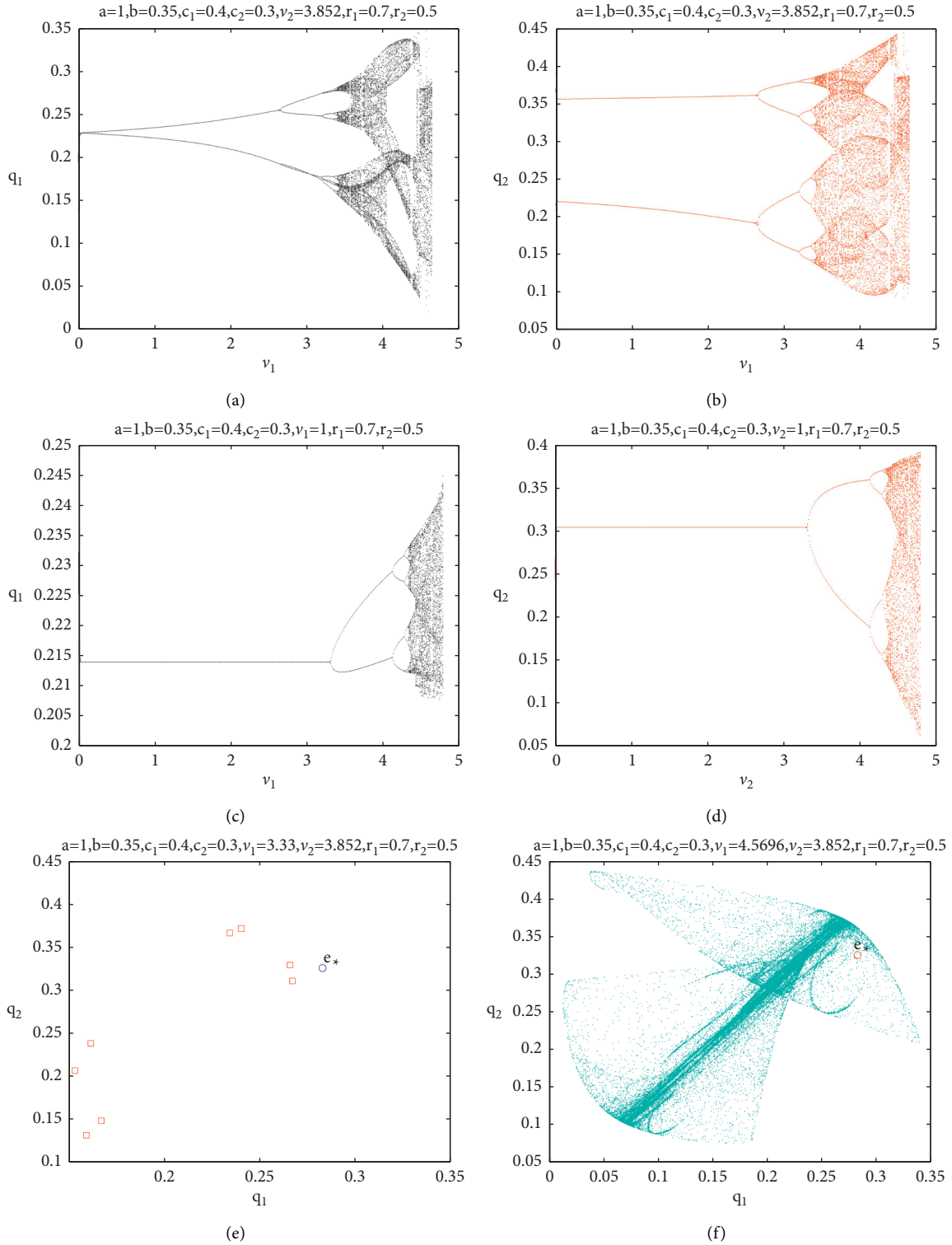

Figure 1: Continued.

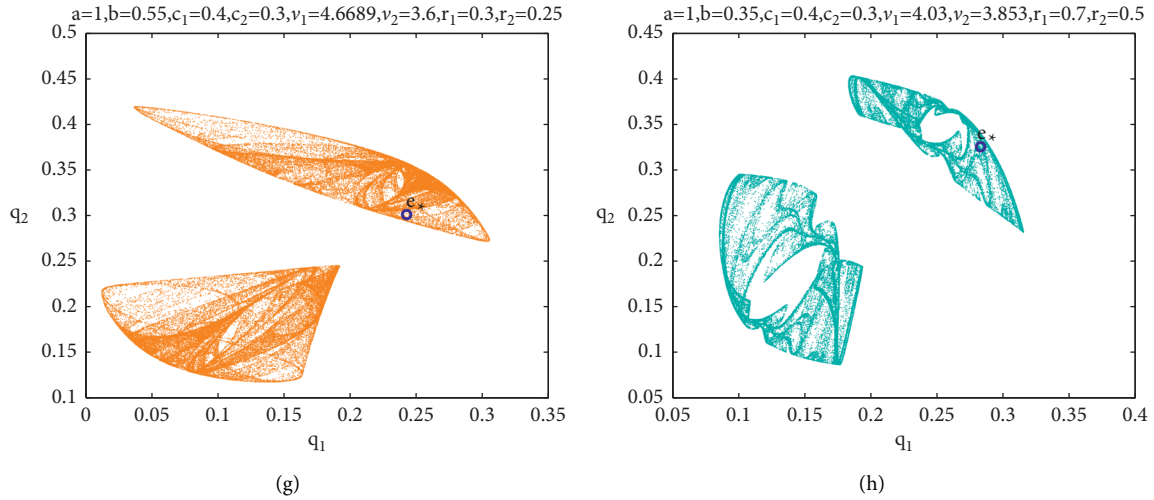

Figure 1: (a)–(d) 1D bifurcation diagram on varying both v_1 and v_2 at $a = 1, b = 0.35, c_1 = 0.4, c_2 = 0.3, r_1 = 0.7, r_2 = 0.5$, and $v_1 = 1$ (or $v_2 = 3.852$) on varying v_2 (or on varying v_1). (e) The phase plane of period-8 cycle at $a = 1, b = 0.35, c_1 = 0.4, c_2 = 0.3$, $r_1 = 0.7, r_2 = 0.5$, $v_1 = 3.33$, and $v_2 = 3.852$. (f) The phase plane of one-piece chaotic attractor at $a = 1, b = 0.35, c_1 = 0.4, c_2 = 0.3, r_1 = 0.7$, $r_2 = 0.5, v_1 = 4.5696$, and $v_2 = 3.852$. (g) Two-piece chaotic attractor at $a = 1, b = 0.55, c_1 = 0.4, c_2 = 0.3, r_1 = 0.3, r_2 = 0.25, v_1 = 4.6689$, and $v_2 = 3.6$. (h) Two-piece chaotic attractor at $a = 1, b = 0.35, c_1 = 0.4, c_2 = 0.3, r_1 = 0.7, r_2 = 0.5, v_1 = 4.03$, and $v_2 = 3.852$.

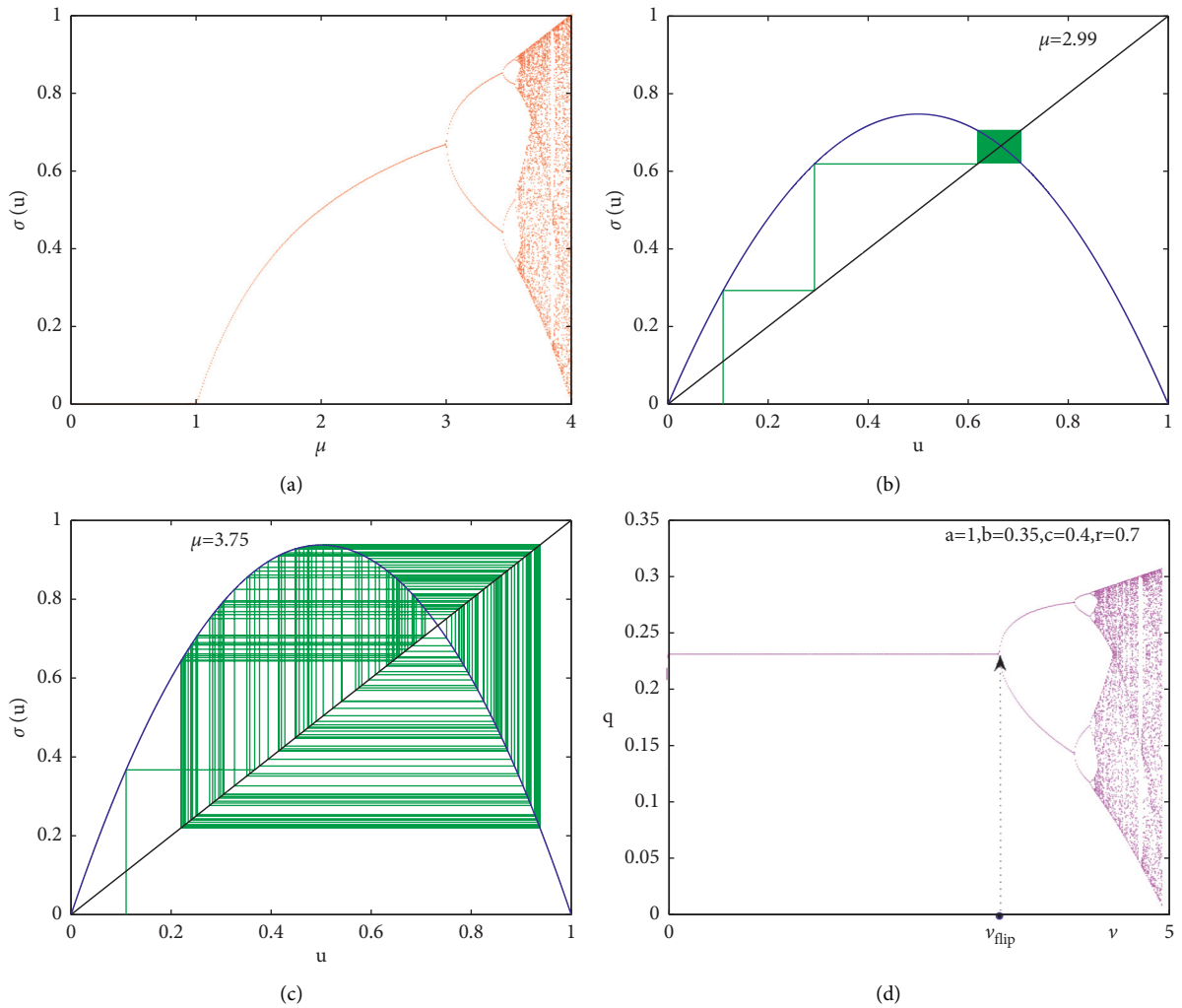

Figure 2: (a) 1D bifurcation diagram of map $\sigma(u)$ with respect to $\mu 1$. Iterations of $\sigma(\mu)$ at (b) $\mu = 2.99$ and (c) $\mu = 3.75$. (d) 1D bifurcation diagram for the map (14) at $a = 1$, $b = 0.35$, $c = 0.4$, and $r = 0.7$.

the restriction imposed on Δ will be described by the one-dimensional map given below.

$$T_\Delta\colon q' = g(q) \coloneqq q + \nu q[a - c - (2 + b(1 + r_1))q]. \quad (14)$$

That is to say, any synchronized trajectories (i.e., $q_1(t) = q_2(t)$ for every time step t) will be governed by $T_\Delta\colon \Delta \longrightarrow \Delta$, and the following proposition is raised.

Proposition 7. *The map (14) is unimodal and concave,* $\lim_{q\longrightarrow 0^+} g(q) = 0$, *and* $\lim_{q\longrightarrow+\infty} g(q) = -\infty$. *This means that there is a threshold* $\overline{q} = 1 + \nu(a - c)/\nu[2 + b(1 + r)]$ *at* $g(\overline{q}) = 0$. *When the model becomes unimodal, one gets the following critical point.*

$$q_{\mathrm{cr}} = \frac{1 + \nu(a - c)}{2\nu[2 + b(1 + r)]}. \quad (15)$$

Proof. The proof is straightforward by looking at the function $g(q)$ that has a global maximum without any local maximum, and hence it is unimodal. The sign of the second derivative of $g(q)$ proves that the map is concave and finally $g'(q_{\mathrm{cr}}) = 0$.

Now, the map T_Δ has only one fixed point, that is, $\overline{q}$, and this point is locally stable if $\nu < 2/a - c$ while flip bifurcation takes place at $\nu = \nu_{\mathrm{flip}}\colon = 2/a - c$. Figure 2(d) shows a 1D bifurcation diagram where flip bifurcation takes place at $\nu \approx 3.33$. □

5. Basin of Attraction

Here, some properties of the map (7) regarding its attractive basin are given. According to [29], it is possible to see that the coordinate axes and their preimages of any rank construct boundaries for initial conditions of any nondiverging trajectories. It can be seen that the dynamics of map (7) can be restricted to the invariant axes and can be rewritten in the one-dimensional map as follows.

$$\acute{q}_i = g_i(q_i) \coloneqq q_i[1 + \nu_i(a - c_i) - 2\nu_i q_i], \quad i = 1, 2, \quad (16)$$

which possesses a positive fixed point, $q_i^* = (1 + \nu_i(a - c_i)/2\nu_i)$, $i = 1, 2$. It is easy to see that $g_i(q_i)$ is concave and increasing function provided that $q_i < 1 + \nu_i(a - c_i)/4\nu_i$. In addition, for any points in the form $(q_1, 0), q_1 > 0$, or $(0, q_2), q_2 > 0$, one gets s or $\acute{q}_1 = 0, \acute{q}_2 > 0$. Conversely, if $q_i > 1 + \nu_i(a - c_i)/4\nu_i$, then $g_i(q_i)$ is concave and unimodal. In the last case, one can get the nonnegative points $\widetilde{q}_i^{\mathrm{bound}} = 1 + \nu_i(a - c_i)/2\nu_i$ and $\widetilde{q}_i^{\mathrm{cr}} = 1 + \nu_i(a - c_i)/4\nu_i$ at $\acute{q}_i = 0$ and $\acute{g}_i(\widetilde{q}_i^{\mathrm{cr}}) = 0$, respectively. If $\acute{g}_i(\widetilde{q}_i^{\mathrm{cr}}) < \widetilde{q}_i^{\mathrm{bound}}$, i.e., if $\nu_i(a - c_i) < 3$, this means that trajectories along the invariant axes are bounded if the initial states lie on the line segment $\omega_i = [O, O_i^{-1}], i = 1, 2$, where $O_i^{-1} = \widetilde{q}_i^{\mathrm{bound}} \neq 0$ is the rank-1 preimage of the point of origin. In contrast, any other trajectories along the invariant axes starting from an initial state outside ω_i become unfeasible. Furthermore, calculating the eigenvalues at a generic point (q_1, q_2) on the invariant axis q_i gives $\widetilde{\lambda}_i = 1 + \nu_i(a - c_i) - 4\nu_i q_i$, $i = 1, 2$. This means that trajectories commencing close to these invariant axes with positive initial states are repelled by those axes. In Figure 3(b), the line segments $\omega_i, i = 1, 2$, and their inverses $\omega_i^{-1}, i = 1, 2$, are depicted at the set of parameter values $a = 1, b = 0.35, c_1 = 0.4, c_2 = 0.3, r_1 = 0.7, \ r_2 = 0.5, \nu_1 = 4.5696$, and $\nu_2 = 3.852$ where the point O_3^{-1} is the fourth preimage point of the origin and is given by

$$O_3^{-1} = (\mathring{q}_1, \mathring{q}_2),$$

$$\mathring{q}_1 = \frac{2\nu_2 - b(1 - \alpha_1)\nu_1 + \nu_1\nu_2[2(a - c_1) - b(a - c_2)(1 - \alpha_1)]}{4 - b^2(1 - r_1)(1 - r_2)},$$

$$\mathring{q}_1 = \frac{2\nu_1 - b(1 - \alpha_2)\nu_2 + \nu_1\nu_2[2(a - c_2) - b(a - c_1)(1 - \alpha_2)]}{4 - b^2(1 - r_1)(1 - r_2)}. \quad (17)$$

It is also noted that this point is the intersection of both inverses ω_1^{-1} and ω_2^{-1}.

5.1. Critical Curves. Besides the fact that the map (7) is nonlinear, it is also noninvertible map, which means that the rank-1 preimages of a point (q_1, q_2) may not exist or may be multivalued. As one can see, the origin point possesses four rank-1 preimages, and hence the phase plane of map (7) includes Z_4 zone, the zone whose points have four rank-1 preimages. It may also include Z_2, the zone whose points possess two rank-1 preimages, and Z_0, the zone with no rank-1 preimages. To investigate these zones, let us calculate the rank-1 preimages for the points along the invariant axes and take the forms $(p, 0)$ and $(0, q)$. Substituting these points into the map (7), one gets the following algebraic systems.

$$\begin{aligned} p &= q_1 + \nu_1 q_1[a - c_1 - 2q_1 - b(1 + r_1)q_2], \\ 0 &= q_2 + \nu_2 q_2[a - c_2 - 2q_2 - b(1 + r_2)q_1], \end{aligned} \quad (18a)$$

$$\begin{aligned} 0 &= q_1 + \nu_1 q_1[a - c_1 - 2q_1 - b(1 + r_1)q_2], \\ q &= q_2 + \nu_2 q_2[a - c_2 - 2q_2 - b(1 + r_2)q_1]. \end{aligned} \quad (18b)$$

Solving the second equation of (18a) gives the following: $q_2 = 0$ or $0 = 1 + \nu_2[a - c_2 - 2q_2 - b(1 + r_2)q_1]$, and then one gets two case.

Case 1. Substituting $q_2 = 0$ in the first equation of (18a) gives the following quadratic equation.

$$2\nu_1 q_1^2 - (1 + \nu_1(a - c_1))q_1 + p = 0. \quad (19a)$$

This means that the point in the form $(p, 0)$ may have no preimages or two distinct real-1 preimages.

Case 2. At $0 = 1 + \nu_2[a - c_2 - 2q_2 - b(1 + r_2)q_1]$, one gets the algebraic system

$$\begin{aligned} p &= q_1 + \nu_1 q_1[a - c_1 - 2q_1 - b(1 + r_1)q_2], \\ 0 &= 1 + \nu_2[a - c_2 - 2q_2 - b(1 + r_2)q_1]. \end{aligned} \quad (19b)$$

Solving (19b), we get the following quadratic equation.

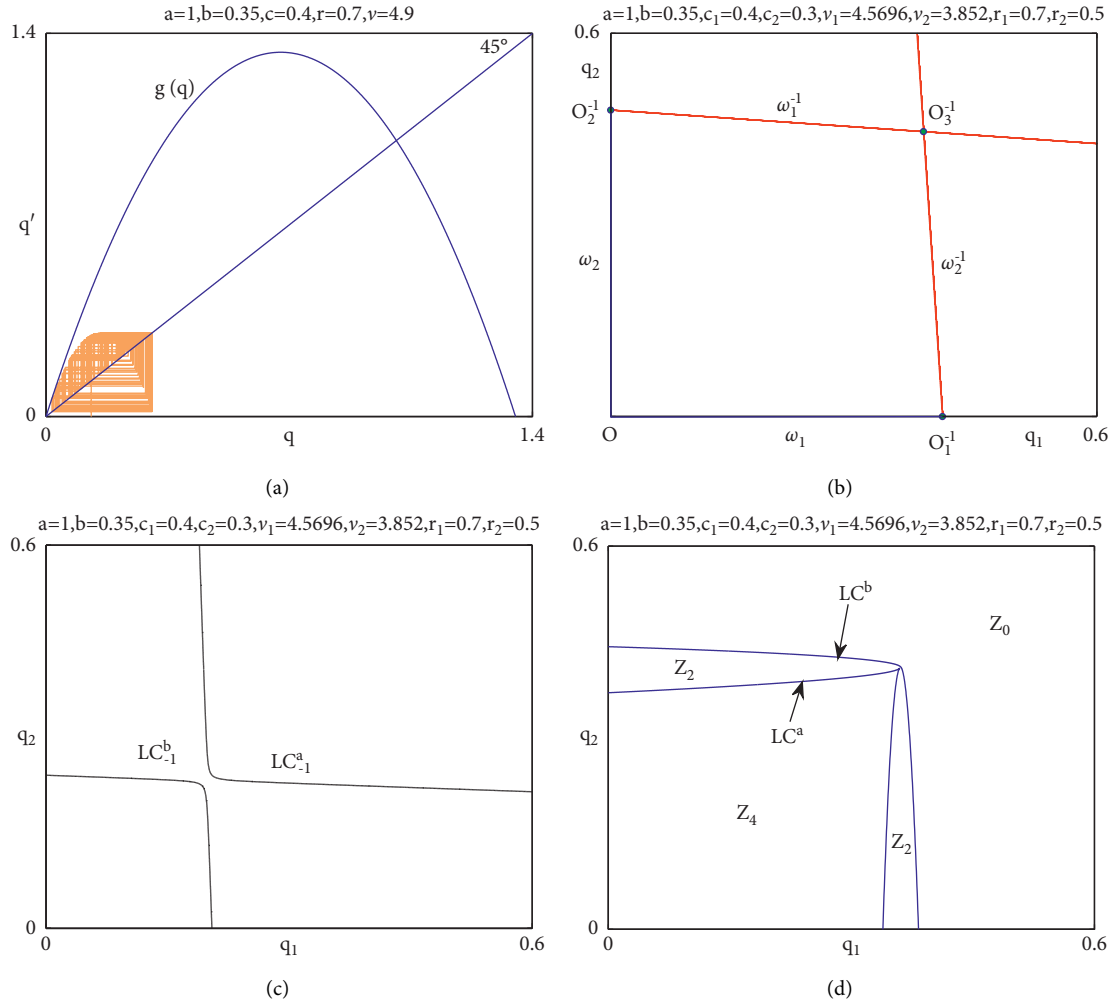

FIGURE 3: (a) The shape of map T_Δ at the values $a = 1, b = 0.35, c = 0.4, r = 0.7,$ and $v = 4.9$. At $a = 1, b = 0.35, c_1 = 0.4, c_2 = 0.3, r_1 = 0.7, r_2 = 0.5, v_1 = 4.5696,$ and $v_2 = 3.852 v_2 = 3.852$. (b) The segments $\omega_i, i = 1, 2,$ and their inverses ω_i^{-1}. (c)-(d) The locus LC_{-1} and the critical curve LC with the corresponding zones.

$$v_1\left[4 - b^2(1 - r_1)(1 - r_2)\right]q_1^2 - 2\left[(a - c_1)v_1 - \frac{b}{2}(1 - r_1)(1 + (a - c_2)v_1)\right]q_1 + p = 0. \tag{19c}$$

This means that in this case, the point $(p, 0)$ may have no preimages or two distinct real rank-1 preimages. Combining the two cases, one can conclude that such points in the invariant axes may have four, two, or no preimages. For the interior points in the form $(p, q) \neq (0, 0)$, it is complicated to categorize such points as belonging to one of the zones $Z_0, Z_2,$ or Z_4 due to the difficulty of solving the algebraic system (18a) at this point. For this reason, numerical simulation is used to calculate critical curves. The critical curves are responsible for dividing the map's phase plane into these zones. The critical curve of rank-1 is denoted by LC and forms a locus of coincident points of rank-1 preimages located on a set denoted by LC_{-1}. Since the map (7) is continuously differentiable, LC_{-1} can be defined as the locus of points where the associated Jacobian determinant is vanished; i.e., $LC_{-1} \subseteq \{(q_1, q_2) \in \mathbb{R}^2 : \det(J(q_1, q_2)) = 0\}$, where $J(q_1, q_2)$ is defined by (A.1) in the appendix. Therefore, LC represents the rank-1 image of LC_{-1} under the map T given in (7); i.e., $LC = T(LC_{-1})$. The expression for $\det(J(q_1, q_2)) = 0$ is cumbersome and is omitted here, and we instead do numerical simulation for presenting both LC_{-1} and LC. Figure 3(c) shows that LC_{-1} consists of two branches LC_{-1}^a and LC_{-1}^b while Figure 3(d) presents the critical curve that is also formed by two branches, LC^a and LC^b. It is also clear that the map (7) is not invertible as its phase plane is divided into three zones, $Z_0, Z_2,$ and Z_4.

6. Global Analysis

In economic models, global analysis is required to investigate the topological structure of basin of attraction that is not recognized by local analysis and whose qualitative changes occur due to change in parameter values. The long-term behavior of variables of these economic models given initial

conditions is indeed necessary in order to show the influences that may result if these initials are taken far away from a fixed point of an attracting set. The numerical analysis shows two important aspects for the map (7), the asymmetric and symmetric cases. Let us first begin analyzing the asymmetric case by adopting the following set of parameter values: $a = 1, b = 0.35, c_1 = 0.4, c_2 = 0.3, r_1 = 0.7, r_2 = 0.5$, $\nu_1 = 3.3285$, and $\nu_2 = 3.852$. This set is given in Figure 4(a) which represents a period-8 cycle with Nash equilibrium point and its attractive basins. These basins are colored orange and green while the escaping (or infeasible points) domain is plotted in gray color. It is also clear that the escaping domain forms a connecting set. By increasing the speed parameter of the first firm to $\nu_1 = 4.03$ while keeping the other values fixed, the dynamic of map (7) turns to a chaotic attractor that consists of two disconnecting areas as shown in Figure 4(b). It can be observed that the branch LC^b of the critical curve LC is moving upward. With further increase in this parameter to $\nu_1 = 4.4675$, a one-piece chaotic attractor emerges in Figure 4(c). Its attracting domain is displayed in white color and is separated from the infeasible domain by the segments ω_1^{-1} and ω_2^{-1}. At $\nu_1 = 4.647$, with the other parameter values being fixed, the chaotic attractor continues to appear, the critical curve LC^b becomes tangent to the boundary ω_2^{-1}, and hence contact bifurcation is raised as given in Figure 4(d). This contact takes place only when one branch LC^b of the critical curve which separates Z_2 zone from Z_0 zone becomes tangent to ω_2^{-1}. This contact with the boundary of infeasible domain occurs from one side due to asymmetry between the two branches of map (7). This contact bifurcation becomes more visible in Figure 4(e) at the parameters set $\nu_1 = 4.63$ and $\nu_2 = 3.95$ while the other parameters are fixed. As one can see, the contact bifurcation causes disconnection in the infeasible domain because an area h_0 from Z_0 zone moves into Z_2 zone; i.e., $LC^b \cap \omega_2^{-1} = h_0$, which is out of the quadrilateral $OO_1^{-1}O_3^{-1}O_2^{-1}$. This kind of contact bifurcation is well-known (see [29]). Just after it, the area h_0 from the infeasible domain enters inside the region Z_2. As a result, the points belonging to this region have now two distinct preimages. Since this region belongs to Z_0, their preimages will belong to the same region and form holes lying in the attraction domain that is bounded by the quadrilateral shape $OO_1^{-1}O_3^{-1}O_2^{-1}$. Indeed, only at $\nu_i = 2/(a - c_i), i = 1$, both h_0 and its preimage h_0^{-1} (that is formed by two areas connected by the branch LC_{-1}^b) have a contact with coordinate axes. It is also clear that both h_0 and h_0^{-1} are entirely located in the region Z_2. Therefore, each of them has further preimages that form smaller holes of the infeasible domain located in the attracting domain and are bounded by rank-2 preimages of the segments ω_1 and ω_2.

In contrast, the symmetric case is now investigated. This case happens at $\nu_1 = \nu_2 = \nu, c_1 = c_2 = c$, and $r_1 = r_2 = r$. This means the map (7) can be rewritten in the following form.

$$T_*(q_1, q_2): \begin{cases} q_1(t+1) = q_1(t) + \nu q_1(t)\left[a - c - 2q_1(t) - b(1+r)q_2(t)\right], \\ q_2(t+1) = q_2(t) + \nu q_2(t)\left[a - c - 2q_2(t) - b(1+r)q_1(t)\right]. \end{cases} \tag{20}$$

The map (20) is symmetric on the diagonal Δ, and studying its dynamics through local analysis around Δ is related to synchronization (intermittency). In this regard, one can say that a dynamic behavior of the map is synonymized if there exists a step time $\mathring{t}$ such that $q_1(t) = q_2(t)$ for any $t > \mathring{t}$. Therefore, in this case, the dynamics can be studied by recalling the Jacobian of map (20) given by

$$J(q_1, q_2) = \begin{pmatrix} \ell(q) & m(q) \\ m(q) & \ell(q) \end{pmatrix}, \tag{21}$$

where, $\ell(q) = 1 + \nu[a - c - (4 + (1+r)b)q]$ and $m(q) = -b(1+r)\nu q$. Then, the eigenvalues can be given as follows.

$$\begin{aligned} \lambda_{\parallel} &= \ell(q) + m(q) = 1 + \nu[a - c - 2(2 + (1+r)b)q], \\ \lambda_{\perp} &= \ell(q) - m(q) = 1 + \nu(a - c - 4q), \end{aligned} \tag{22}$$

and their corresponding eigenvectors are $(1, 1)$ and $(1, -1)$, respectively. In this case, $e_* = (a - c/2 + b(1+r), a - c/2 + b(1+r))$, and then the following proposition is raised.

Proposition 8. *The point e_* is locally stable provided that $\nu < 2/a - c$. At $\nu = \nu_f = 2/a - c$, the point e_* undergoes flip bifurcation.*

Proof. Substituting e_* into (22), we get

$$\begin{aligned} \lambda_{\parallel} &= 1 - \frac{(a-c)[2 - (1+r)b]}{2 + b(1+r)}\nu, \\ \lambda_{\perp} &= 1 + \nu(a - c). \end{aligned} \tag{23}$$

Simple calculations make $|\lambda_{\perp}| < 1$ if $\nu < 2/a - c$, and $|\lambda_{\parallel}| < 1$ if $\nu < 2[2 + (1+r)b]/(a-c)[2 - (1+r)b]$. Combining the two conditions on ν gives $\nu < 2/a - c$, and this completes the proof.

From the above proposition, one can deduce that the parameter ν plays a key role in the stability of e_*. This means that high reactivity of each firm with respect to a marginal change in its average profit should exist. Furthermore, the importance of the above proposition comes from its generalization when an attracting cycle for the map T_* on Δ exists. To see that, suppose that a k-cycle given by

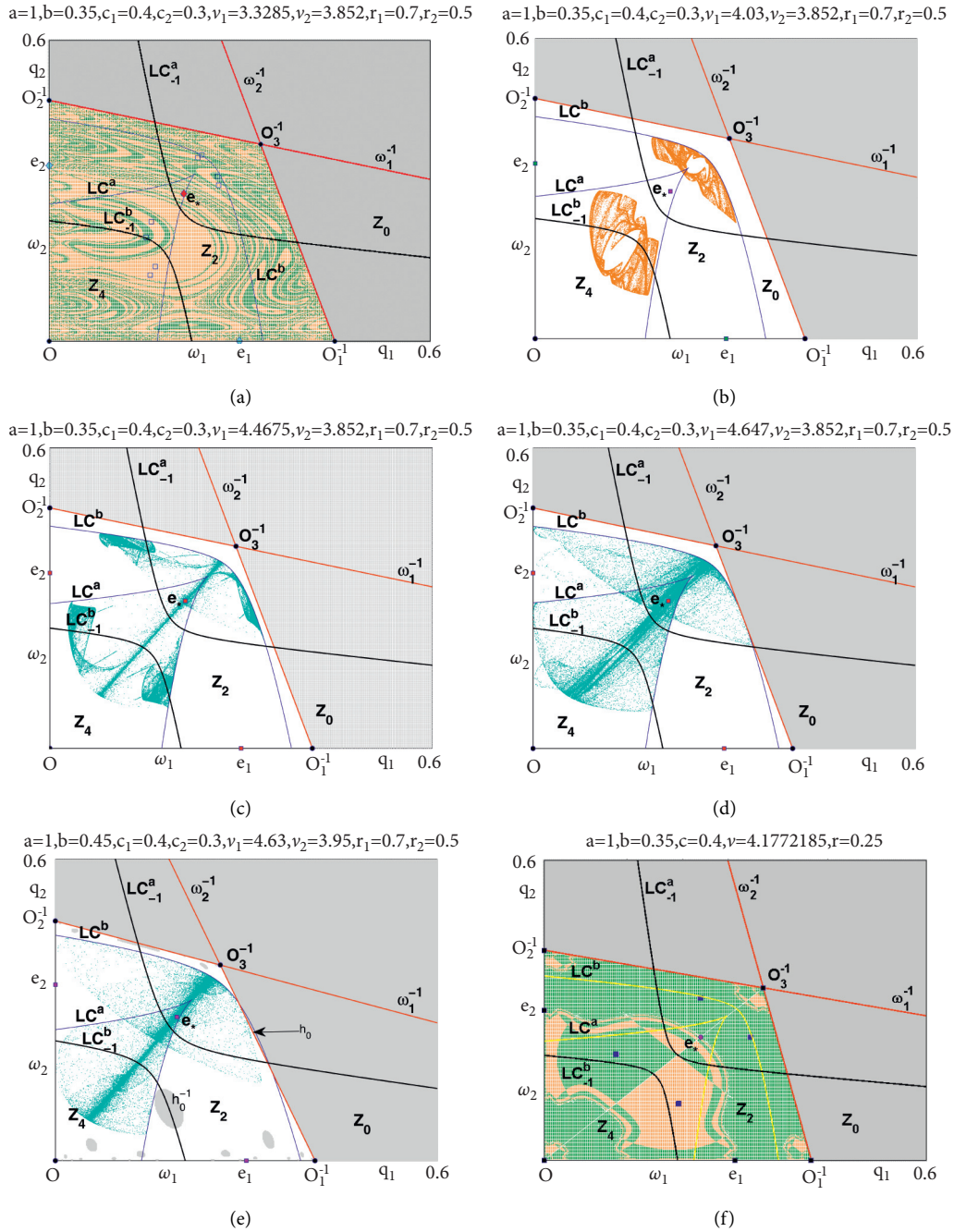

Figure 4: Continued.

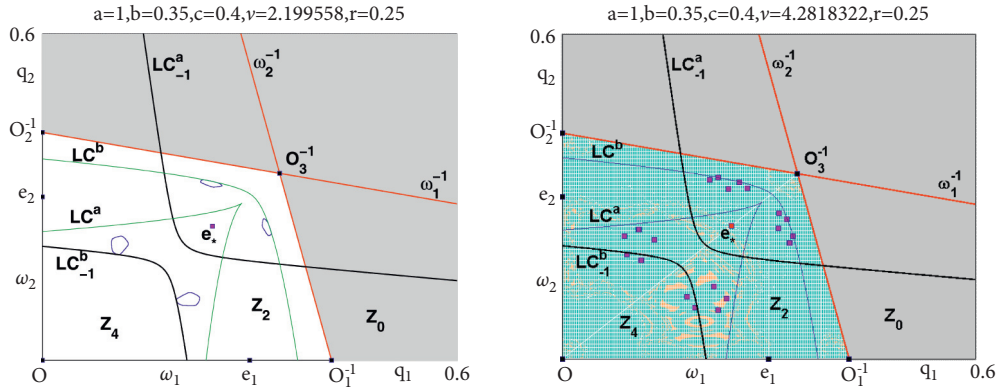

(g) (h)

Figure 4: At $a = 1, b = 0.35, c_1 = 0.4, c_2 = 0.3, r_1 = 0.7, r_2 = 0.5$, the basin of attraction for (a) period-8 cycle, $\nu_1 = 3.3285, \nu_2 = 3.852$. (b) Two-piece chaotic attractor, $\nu_1 = 4.03, \nu_2 = 3.852$. (c) One-piece chaotic attractor, $\nu_1 = 4.4675, \nu_2 = 3.852$. (d) One-piece chaotic attractor, $\nu_1 = 4.647, \nu_2 = 3.852$. (e) One-piece chaotic attractor, $\nu_1 = 4.63, \nu_2 = 3.3.95$. At $a = 1, b = 0.35, c = 0.4, r = 0.25$, the basin of attraction for (f) period-4 cycle, $\nu = 4.1772185$. (g) Four closed rings, $\nu = 4.2199558$. (h) Period-20 cycle, $\nu = 4.2818322$.

$\{(q_1, q_1), \ldots, (q_m, q_m)\}$ of the map T_* is embedded in the invariant diagonal Δ which corresponds to the cycle $\{q_1, \ldots, q_m\}$. Then, the multipliers for this k-cycle are given by

$$\lambda_{\parallel}^{k} = \prod_{i=1}^{k} (\ell(q_i) + m(q_i)),$$
$$\lambda_{\perp}^{k} = \prod_{i=1}^{k} (\ell(q_i) - m(q_i)), \tag{24}$$

whose eigenvectors are $(1, 1)$ and $(1, -1)$. As shown, the stability of e_* is governed by $|\lambda_{\perp}| < 1$ and is confirmed by $|\lambda_{\parallel}| < 1$. In contrast, a complex chaotic attractor H for the map T_* says that H is asymptotically stable if and only if all trajectories belonging to H are transversely attracting. This asymptotic stability condition of H is given in terms of transverse Lyapunov exponent as follows.

$$\Lambda_{\perp} = \lim_{n \longrightarrow \infty} \sum_{i=1}^{n} \ln|\lambda_{\perp}(q(i))|, \tag{25}$$

where $q(0) \in H$ and $q(i)$ is the trajectories generated by the map

$$T_s: q(t+1) = q(t) + \nu q(t)[a - c - (2 + b(1 + r)q(t))]. \tag{26}$$

The following definitions are given [29]. □

Definition 1. A chaotic attractor H is asymptotically stable if it is Lyapunov stable; i.e., for every neighborhood U of H, there exists a neighborhood V of H such that $T^n(V) \subset U \forall n \geq 0$ and the attractive basin $B(H)$ possesses a neighborhood of H.

A spectrum of Lyapunov exponents can be defined according to the initial conditions as follows [30].

$$\Lambda_{\perp}^{\min} < \cdots < \Lambda_{\perp}^{\text{nat}} < \cdots < \Lambda_{\perp}^{\max}, \tag{27}$$

where $\Lambda_{\perp}^{\text{nat}}$ denotes a Lyapunov exponent evaluated at a generic trajectory in the chaotic attractor H. If $\Lambda_{\perp}^{\max}$ is nonpositive, then a set is called Lyapunov attractor. While $\Lambda_{\perp}^{\max} > 0$ and $\Lambda_{\perp}^{\text{nat}} < 0$, the set becomes no longer Lyapunov stable and becomes Milnor attractor. It is defined as follows.

Definition 2. A closed invariant set H is called a weak attractor in Milnor sense if its stable set (the basin of attraction) $B(H)$ has positive Lebesgue measure.

Now, we give some experiments through numerical analysis to confirm the above findings. Let us assume the following set: $a = 1, b = 0.35, c = 0.4, \nu = 4.1772185$, and $r = 0.25$. At this set, the dynamic of map (20) is represented by period-4 cycle given in Figure 4(f). Its attractive basin and the basin of Nash equilibrium point are colored green and orange, respectively, and are bounded by ω_1 and ω_2 and their inverses. The infeasible domain of this cycle is given in gray color. By keeping the same set of values and increasing ν to 4.2199558, four closed invariant rings emerge around the diagonal as depicted in Figure 4(g). All these rings are symmetric around the invariant diagonal Δ and lie within the region Z_2 only when two of them are tangent to the branch of critical curve LC^b. By further increasing ν to 4.2818322, the four rings convert into a period-20 cycle as shown in Figure 4(h) whose basin of attraction is colored cyan while the basin of Nash point is denoted by orange color. At $\nu = 4.414216$, while the other parameter values are fixed, a Milnor attractor is raised on the invariant diagonal as presented in Figure 5(a). This means the dynamics of map (20) are captured by a two-piece chaotic attractor on the invariant diagonal Δ that is in Milnor sense. This indicates that any cycle embedded in the diagonal Δ is transversely unstable, and hence all trajectories approaching that diagonal are exploded away by transversely unstable cycles. By further increasing ν to 4.763885, a one-piece chaotic attractor emerges as shown in Figure 5(b). This chaotic attractor is symmetric on the diagonal because synchronization still occurs. The symmetry of this chaotic attractor is

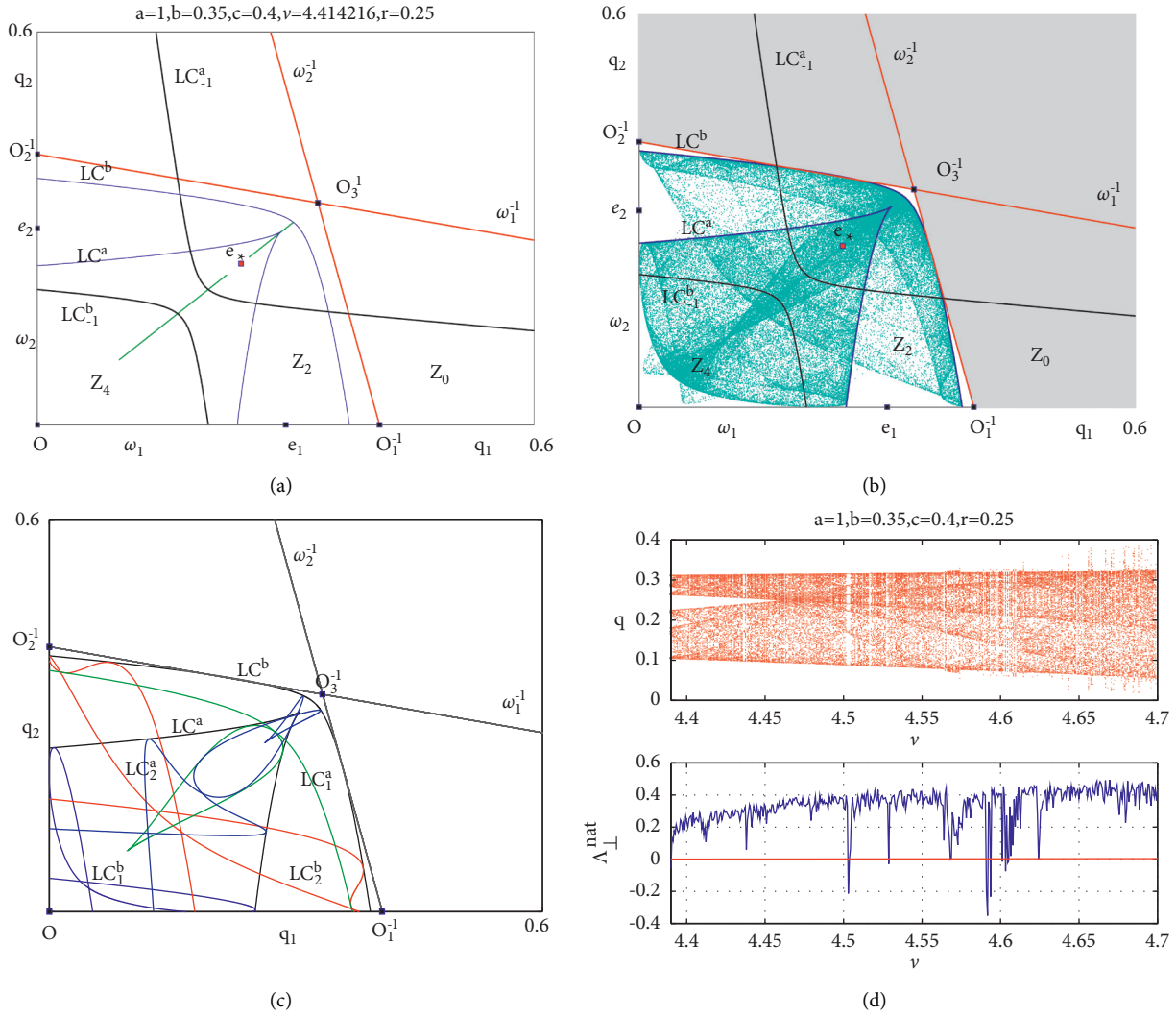

FIGURE 5: At $a = 1, b = 0.35, c = 0.4, r = 0.25$, the basin of attraction for (a) Milnor attractor, $\nu = 4.414216$. (b) One-piece chaotic attractor, $\nu = 4.763885$. (c) The boundaries of chaotic attractor in (b). (d) Bifurcation diagram on varying ν and the corresponding transverse Lyapunov exponent for $\nu \in [4.4, 4.7]$.

given in Figure 5(c) where its boundary at the same set of parameter values is given by the critical curves $LC^a, LC^b, LC^a_1, LC^b_1, LC^a_2$, and LC^b_2. In Figure 5(d), the transverse Lyapunov exponent is given. It gives better understanding on the map's dynamics in the long term. As one can see, the bifurcation diagram corresponding to the transverse Lyapunov exponent confirms the existence of chaotic attractor on the invariant diagonal in the interval $\nu \in [4.4, 4.7]$ except for windows of some periodic cycles. It is also noted that in this interval of the speed parameter ν, the Lyapunov exponent changes its sign many times until it eventually becomes positive for large values of the speed parameter ν. From economic perspective, this implies that the long-term dynamics of the map (20) can be very sharp due to small changes in this parameter. In other words, firms commencing with the same initial states may be different in the long term.

7. Conclusion

In this paper, some dynamic characteristics such as multistability, synchronization phenomena, and complex structure of some attractive basins are investigated for a nonlinear two-dimensional noninvertible map describing a Cournot duopoly game with an invariant one-dimensional manifold where synchronization takes place. It has been proved that, with identical firms, the game's map becomes symmetric and both coordinate axes and diagonal $q_1 = q_2$ form invariant manifolds. The main results in this paper concern the global analysis in the asymmetric and symmetric case where synchronization has taken place. Such global analysis has focused on the properties of critical curves of the noninvertible map. The phase plane of game's map has been divided into three zones of preimages, that is, Z_0, Z_2, and Z_4. We have shown that for a set of parameter values, the one-

dimensional Milnor attractor to which the synchronized trajectories arise has been obtained. After that, for increasing the value of the speed parameter, the Milnor attractor is transformed into a chaotic attractor. Indeed, weak chaotic attractor in the Milnor sense has been confirmed by transverse Lyapunov exponent.

Appendix

The Jacobian of map (7) is given by

$$J(q_1,q_2)=\begin{pmatrix} 1+\nu_1[a-c_1-4q_1-b(1-r_1)q_2] & -b\nu_1(1-r_1)q_1 \\ -b\nu_2(1-r_2)q_2 & 1+\nu_2[a-c_2-4q_2-b(1-r_2)q_1] \end{pmatrix}. \tag{A.1}$$

Proof of Proposition 1. At e_o, the above Jacobian matrix becomes

$$J(q_1,q_2)=\begin{bmatrix} 1+\nu_1(a-c_1) & 0 \\ 0 & 1+\nu_2(a-c_2) \end{bmatrix}, \tag{A.2}$$

and hence the eigenvalues are $\lambda_i = 1+\nu_i(a-c_i), i=1,2$. It is clear that $|\lambda_i|>1, i=1,2$, and then e_o is unstable node. □

Proof of Proposition 2. At e_1, the Jacobian matrix (A.1) takes the form

$$J(q_1,q_2)=\begin{bmatrix} 1+\nu_1(a-c_1) & -\dfrac{b}{2}(1-r_1)(a-c_1)\nu_1 \\ 0 & 1+\nu_2\left[a-c_2-\dfrac{b}{2}(1+r_2)(a-c_1)\right] \end{bmatrix}, \tag{A.3}$$

and then the eigenvalues become

$$\begin{aligned} \lambda_1 &= 1-(a-c_1)\nu_1, \\ \lambda_2 &= 1+\nu_2\left[a-c_2-\frac{b}{2}(1+r_2)(a-c_1)\right]. \end{aligned} \tag{A.4}$$

One can see that $|\lambda_1|<1$ gives $0<\nu_1<2/a-c_1$ and $|\lambda_2|<1$ is attainable if $a-c_2<b/2(1+r_2)(a-c_1)$; then, e_1 is stable. If $a-c_2>b/2(1+r_2)(a-c_1)$, one gets $\lambda_2>1$; therefore, e_1 becomes unstable saddle point. □

Proof of Proposition 3. The proof is similar to that of Proposition 1. □

Proof of Proposition 4. Jacobian (A.1) at Nash point e_* has a trace τ and determinant δ given by

$$\begin{aligned} \tau &= 2(1-A\nu_1-B\nu_2), \\ \delta &= 1-2A\nu_1-2B\nu_2+4AB\nu_1\nu_2-b^2AB(1+r_1)(1+r_2). \end{aligned} \tag{A.5}$$

Then, Jury conditions can be obtained as follows.

$$1-\tau+\delta = 4AB\nu_1\nu_2+b^2AB(1+r_1)(1+r_2), \tag{A.6a}$$

$$\begin{aligned} 1+\tau+\delta = {} & 4(1-A\nu_1-B\nu_2+AB\nu_1\nu_2) \\ & -b^2AB(1+r_1)(1+r_2), \end{aligned} \tag{A.6b}$$

$$1-\delta = 2(A\nu_1+B\nu_2-2AB\nu_1\nu_2)+b^2AB(1+r_1)(1+r_2). \tag{A.6c}$$

Since $a>c_1,c_2$ and $a>b$, then the multiplication AB is always nonnegative, and then condition (A.6a) is always positive. Suppose that conditions (A.6b) and (A.6c) are nonnegative; then, combining them gives $0<2A\nu_1+2B\nu_2-4AB\nu_1\nu_2+b^2(1+r_1)(1+r_2)AB<4$, and hence Nash point is stable. The proof is completed. □

Proof of Proposition 5. Jacobian (A.1) at Nash point e_* has two eigenvalues taking the following form.

$$\lambda_{1,2} = 1-A\nu_1-B\nu_2 \pm \sqrt{(A\nu_1-B\nu_2)^2+b^2AB(1+r_1)(1+r_2)}. \tag{A.7}$$

These eigenvalues are real since $AB>0, b>0$, and $(1+r_1)(1+r_2)>0$. Then, the Nash point loses its stability through flip bifurcation only. □

Data Availability

The data are included in the manuscript.

Conflicts of Interest

The author declares no conflicts of interest regarding the content of this article.

Acknowledgments

This research was supported by Project no. RSP-2022/167, King Saud University, Riyadh, Saudi Arabia.

References

[1] T. Puu, "Chaos in duopoly pricing," *Chaos, Solitons & Fractals*, vol. 1, no. 6, pp. 573–581, 1991.

[2] C. H. Tremblay and V. J. Tremblay, "The Cournot-Bertrand model and the degree of product differentiation," *Economics Letters*, vol. 111, no. 3, pp. 233–235, 2011.

[3] D. Rand, "Exotic phenomena in games and duopoly models," *Journal of Mathematical Economics*, vol. 5, no. 2, pp. 173–184, 1987.

[4] J. Tuinstra, "A price adjustment process in a model of monopolistic competition," *International Game Theory Review*, vol. 6, no. 3, pp. 417–442, 2004.

[5] M. Ueda, "Effect of information asymmetry in Cournot duopoly game with bounded rationality," *Applied Mathematics and Computation*, vol. 362, Article ID 124535, 2019.

[6] N. Singh and X. Vives, "Price and quantity competition in a differentiated duopoly," *The RAND Journal of Economics*, vol. 15, no. 4, pp. 546–554, 1984.

[7] S. S. Askar and A. Al-khedhairi, "Dynamic investigations in a duopoly game with price competition based on relative profit and profit maximization," *Journal of Computational and Applied Mathematics*, vol. 367, Article ID 112464, 2020.

[8] S. S. Askar, "On Cournot-Bertrand competition with differentiated products," *Annals of Operations Research*, vol. 223, no. 1, pp. 81–93, 2014.

[9] S. S. Askar, "Tripoly Stackelberg game model: one leader versus two followers," *Applied Mathematics and Computation*, vol. 328, pp. 301–311, 2018.

[10] S. S. Askar and A. Al-Khedhairi, "Analysis of nonlinear duopoly games with product differentiation: stability, global dynamics, and control," *Discrete Dynamics in Nature and Society*, vol. 2017, Article ID 2585708,, 13 pages, 2017.

[11] S. Bylka and J. Komar, "Cournot-Bertrand mixed oligopolies," in *Warsaw Fall Seminars in Mathematical Economics 1975. Lecture Notes in Economics and Mathematical Systems*, M. Łoś, J. Łoś, and A. Wieczorek, Eds., vol. 133, 1976.

[12] J. Häckner, "A note on price and quantity competition in differentiated oligopolies," *Journal of Economic Theory*, vol. 93, no. 2, pp. 233–239, 2000.

[13] P. Zanchettin, "Differentiated duopoly with asymmetric costs," *Journal of Economics and Management Strategy*, vol. 15, no. 4, pp. 999–1015, 2006.

[14] A. Arya, B. Mittendorf, and D. E. M. Sappington, "Outsourcing, vertical integration, and price vs. quantity competition," *International Journal of Industrial Organization*, vol. 26, no. 1, pp. 1–16, 2008.

[15] A. A. Elsadany, "Dynamics of a Cournot duopoly game with bounded rationality based on relative profit maximization," *Applied Mathematics and Computation*, vol. 294, pp. 253–263, 2017.

[16] A. K. Naimzada and F. Tramontana, "Dynamic properties of a Cournot-Bertrand duopoly game with differentiated products," *Economic Modelling*, vol. 29, no. 4, pp. 1436–1439, 2012.

[17] J. Ma, L. Sun, S. Hou, and X. Zhan, "Complexity study on the Cournot-Bertrand mixed duopoly game model with market share preference," *Chaos: An Interdisciplinary Journal of Nonlinear Science*, vol. 28, no. 2, Article ID 023101, 2018.

[18] E. Ahmed, A. S. Hegazi, M. F. Elettreby, and S. S. Askar, "On multi-team games," *Physica A: Statistical Mechanics and its Applications*, vol. 369, no. 2, pp. 809–816, 2006.

[19] E. Ahmed and M. F. Elettreby, "Controls of the complex dynamics of a multi-market Cournot model," *Economic Modelling*, vol. 37, pp. 251–254, 2014.

[20] Y. Peng and Q. Lu, "Complex dynamics analysis for a duopoly Stackelberg game model with bounded rationality," *Applied Mathematics and Computation*, vol. 271, pp. 259–268, 2015.

[21] F. Tramontana, "Heterogeneous duopoly with isoelastic demand function," *Economic Modelling*, vol. 27, no. 1, pp. 350–357, 2010.

[22] J. Tanimoto, *Evolutionary Games with Sociophysics*, Springer, Berlin, Heidelberg, 2019.

[23] J. Tanimoto, *Fundamentals of Evolutionary Game Theory and its Applications*, Springer, Berlin, Heidelberg, 2015.

[24] J. Tanimoto, *Mathematical Analysis of Environmental System*, Springer, Berlin, Heidelberg, 2014.

[25] W. Zhong, S. Kokubo, and J. Tanimoto, "How is the equilibrium of continuous strategy game different from that of discrete strategy game?" *Biosystems*, vol. 107, no. 2, pp. 88–94, 2012.

[26] S. Kokubo, Z. Wang, and J. Tanimoto, "Spatial reciprocity for discrete, continuous and mixed strategy setups," *Applied Mathematics and Computation*, vol. 259, pp. 552–568, 2015.

[27] H. Wang and J. Ma, "Complexity analysis of a Cournot-Bertrand duopoly game model with limited information," *Discrete Dynamics in Nature and Society*, vol. 2013, Article ID 287371, 6 pages, 2013.

[28] F. Cavalli, A. Naimzada, and F. Tramontana, "Nonlinear dynamics and global analysis of a heterogeneous Cournot duopoly with a local monopolistic approach versus a gradient rule with endogenous reactivity," *Communications in Nonlinear Science and Numerical Simulation*, vol. 23, no. 1-3, pp. 245–262, 2015.

[29] G.-I. Bischi, L. Stefanini, and L. Gardini, "Synchronization, intermittency and critical curves in a duopoly game," *Mathematics and Computers in Simulation*, vol. 44, no. 6, pp. 559–585, 1998.

[30] L. Fanti, L. Gori, and M. Sodini, "Nonlinear dynamics in a Cournot duopoly with isoelastic demand," *Mathematics and Computers in Simulation*, vol. 108, pp. 129–143, 2015.